

RSC Advances

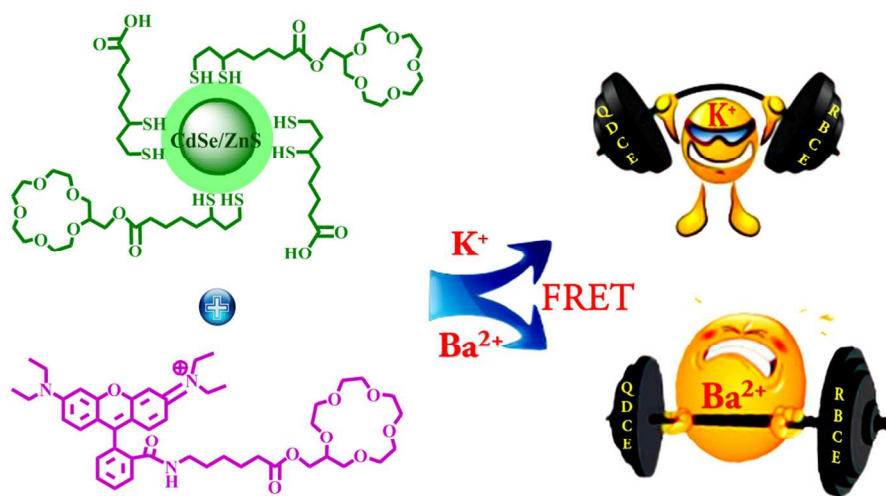


This is an *Accepted Manuscript*, which has been through the Royal Society of Chemistry peer review process and has been accepted for publication.

Accepted Manuscripts are published online shortly after acceptance, before technical editing, formatting and proof reading. Using this free service, authors can make their results available to the community, in citable form, before we publish the edited article. This *Accepted Manuscript* will be replaced by the edited, formatted and paginated article as soon as this is available.

You can find more information about *Accepted Manuscripts* in the [Information for Authors](#).

Please note that technical editing may introduce minor changes to the text and/or graphics, which may alter content. The journal's standard [Terms & Conditions](#) and the [Ethical guidelines](#) still apply. In no event shall the Royal Society of Chemistry be held responsible for any errors or omissions in this *Accepted Manuscript* or any consequences arising from the use of any information it contains.



338x190mm (96 x 96 DPI)

Metal ion Induced Fluorescence Resonance Energy Transfer between Crown Ether Functionalized Quantum dots and Rhodamine B: Selectivity of K⁺ ion

Hsin-Lung Lee,^a Namasivayam Dhenadhayalan^a and King-Chuen Lin*

Department of Chemistry, National Taiwan University, Taipei 106, and
Institute of Atomic and Molecular Sciences, Academia Sinica, Taipei 106, Taiwan.

Abstract

We report a ratiometric fluorescent metal ions sensor based on the mechanism of fluorescence resonance energy transfer (FRET) between synthesized 15-crown-5-ether capped CdSe/ZnS quantum dot (QDCE) and 15-crown-5-ether attached rhodamine B (RBCE) in pH 8.3 buffer solution. Fluorescence titration with different metal ions in pH 8.3 buffer solution of QDCE-RBCE conjugate showed decrease and an increase in the fluorescence intensity for QDCE and RBCE moiety respectively due to FRET from QDCE to RBCE. This sensor system shows excellent selectivity towards K⁺ ion resulted in increasing efficiency of FRET. Energy transfer efficiency depends on the affinity between metal ions and crown ether functionalized with QDCE/RBCE. The detailed analysis of FRET was explored. This water soluble ratiometric sensor system can act as a good FRET probe for sensing applications especially in biological systems.

Keywords: FRET, Metal ion sensor, Quantum dots, Rhodamine B

Introduction

Alkali and alkaline earth metal ions are the most abundant metal ions in physiological systems and necessary for the function of all living cells where they activate many enzymes, participate in the oxidation of glucose to produce adenosine triphosphate and also participate in the transmission of nerve signals.¹ Among them, the importance of K^+ , Na^+ , Mg^{2+} and Ca^{2+} metal ions in biological systems are even more significant.² Potassium ion plays many important roles in the chemical processes of life, including maintenance of ion balance and nerve impulse transmission.³ A deficiency of K^+ ion can cause decreased levels of oxygen, which will reduce the efficiency of cell function. K^+ ion has an essential role in the activation of many growth related enzymes in plants.^{4,5} In Photosynthesis, activation of enzymes by K^+ ion is essential for production of adenosine triphosphate which is an important energy source for many chemical processes taking place in plant issues. Due to their biological and chemical importance so far, several variety of analytical methods have been implemented for the detection of K^+ ions such as fluorescence spectroscopy,⁶ electrochemistry,^{7,8} surface plasmon resonance,⁹ chromatography,^{10,11} colorimetry,¹² and ion-selective electrodes.¹³ Though considerable efforts are being made to develop a simple, sensitive and selective method for K^+ ions detection.

Fluorescence techniques are desirable approaches for the measurement of chemosensors, because this technique is reliable, rapidly performed and highly sensitive.^{14,15} There are different photophysical processes primarily including photoinduced electron or charge transfer, fluorescence resonance energy transfer (FRET), and excimer formation responsible for the photophysical changes (such as fluorescence intensity, spectral changes and lifetimes) upon metal ions binding with fluorophores.¹⁶ Among them, FRET has grown more extensive attentions and promising selectivity and sensitivity.¹⁷ Therefore we have focused on the development of new ratiometric FRET based sensor for metal ions (K^+) in the aqueous medium. For studying the FRET phenomena, energy donor and energy

acceptor must be in close contact to each other. An important type of fluorescent metal ions sensor is based on the molecular recognition of metal ions by crown ethers which were covalently conjugated to fluorophores. Crown ether has been known to form sandwich complex with alkali metal ions and it has tendency to bring the donor and acceptor molecules into close proximity.¹⁸ Various fluorescence sensors such as benzo-15-crown-5 and diaza-18-crown-6 fluoroionophores, pyrenyl-linked benzo-15-crown-5, BODIPY-linked azacrown ethers, benzofuran isophthalate and so on were widely used previously for K^+ ion detection.^{16d,19} With a number of unique optical properties, quantum dots were used as fluorophore for the detection of metal ions based on FRET process.^{20,21} Generally quantum dots can act as energy donors due to their broad absorption band with large absorption cross sections.^{22,23} Previously Chen *et al.* reported that FRET based potassium ion detection by using different size of CdSe/ZnS quantum dots.²¹ There are very few reports to sensing metal ions by using rhodamine-crown ether conjugate.^{24,25}

In the present work, we have synthesized the 15-crown-5-ether attached rhodamine B and 15-crown-5-ether capped CdSe/ZnS quantum dots. In addition, the synthesized QDCE was capped with two different ligands to enhance the solubility of QDs in aqueous solution. The potential application of modified QDs and rhodamine might be controlled as FRET probes to sensing the metal ions. This work aims to probe the effect of alkali and alkaline earth metal ion on the FRET kinetics between QDCE and RBCE. Herein, QDCE and RBCE used as an energy donor and energy acceptor respectively. The study of FRET based metal ion selectivity was performed for QDCE-RBCE conjugate system with various metal ions using fluorescence titration method. The analysis of FRET effect on sensing metal ions was explored in more detailed. Herein, the detection limit of 4.3 μM was obtained for K^+ ion. The determined value for K^+ ion was found to be lower than those reported previously,^{17a,18e,26,27} and close to some earlier literatures.^{17b,21,28,29} Note that the

sensing of K^+ ion by using colorimetric methods exhibited lower detection limit in the nM range.^{30,31}

Results and Discussion

The synthesis of 15-crown-5-ether attached rhodamine B was carried out as shown in Scheme 1. To synthesize the Boc-6-Ahx-15-crown-5 compound (iii), 6-aminohexanoic acid was treated with di-*tert*-butyl dicarbonate (Boc_2O) to protect the amino group in the presence of sodium hydroxide to yield Boc-6-aminohexanoic acid (ii).³² Then 2-hydroxymethyl-15-crown-5-ether (1000 mg, 4 mmol) and 4-dimethylaminopyridine (DMAP, 30 mg, 0.27 mmol) were added to the above solution. The reaction mixture was cooled down to 0 °C. Thereafter, *N,N'*-dicyclohexylcarbodiimide (DCC, 825 mg, 4 mmol) dissolved in dichloromethane (DCM, 15 mL) was slowly added to the mixture. After stirring at room temperature under N_2 atmosphere for 12 h, the solution was filtered and the filtrate was washed with 0.05 N HCl and brine. The organic phase was dried with dry $MgSO_4$ and concentrated in vacuum. The residue was purified by silica gel column chromatography using ethyl acetate/hexanes (1:1, v/v) which afforded the Boc-6-Ahx-15-crown-5 product. The Boc amino protecting group was then removed by trifluoroacetic acid (TFA)/DCM (1:1, v/v) for 1 h, and concentrated in vacuum to give 6-Ahx-15-crown-5 (iv).

The mixture of DCC (144 mg, 0.7 mmol), hydroxybenzotriazole (HOBt, 95 mg, 0.7 mmol) and *N,N*-diisopropylethylamine (DIPEA, 90 mg, 0.7 mmol) in cold DCM were added to a solution of rhodamine B (304 mg, 0.63 mmol) dissolved in cold DCM (2 mL). After 5 min, 6-Ahx-15-crown-5 (254 mg, 0.7 mmol) was added to the above solution. The mixture was stirred at room temperature under N_2 atmosphere for 12 h, the resultant mixture were filtered through a glass frit and concentrated in vacuum to remove the DCM. The residue was dissolved in ethyl acetate and washed with 1 M $K_2CO_{3(aq)}$. The organic phase was dried with dry $MgSO_4$ and concentrated

in vacuum. The residue was purified by silica gel column chromatography using methanol/dichloromethane (1:20 to 1:9, v/v) to afford a pink liquid (214 mg, 41% yield). The final product RBCE was characterized by ^1H , ^{13}C NMR and ESI-MS (Fig. S2, ESI †).

The 15-crown-5-ether capped CdSe/ZnS QDs was synthesized by three steps using the procedure reported by Chen *et al.*²¹ and Mattoussi *et al.*³³ In order to enhance the solubility of QDs in buffer solution, the modification was applied. In the present work, the CdSe/ZnS was capped with dihydrolipoic acid (DHHLA) along with 15-crown-5-ether as illustrated in Scheme 2. At first step, the 15-crown-5-lipoic acid was prepared following literature method.²¹ In brief, lipoic acid (A, 908 mg, 4.4 mmol) was added to a solution of 2-hydroxymethyl-15-crown-5-ether (1 g, 4 mmol) in DCM (15 mL), and stirring for 15 min at 0 °C under N_2 . Then *N*-(3-dimethylaminopropyl)-*N'*-ethylcarbodiimide (EDC) (0.77 mL, 4.4 mmol) and DMAP (49 mg, 0.4 mmol) were added into above solution. The reaction mixture was stirred for 18 h under N_2 at room temperature, the resulting mixture was washed with Millipore water and brine. The organic phase was dried with dry MgSO_4 and concentrated in vacuum. The residue was purified by silica gel column chromatography using ethyl acetate/hexanes (1:1, v/v) to afford a yellow liquid (1.8 g, 93% yield). In the second step, 15-crown-5-DHHLA (C) and DHHLA (D) was prepared by sodium borohydride reduction method. 15-crown-5-DHHLA was characterized by ^1H , ^{13}C NMR and MS (Fig. S3, ESI †). Finally, 5 μL of each 15-crown-5-DHHLA and DHHLA (1:1, v:v) was mixed with CdSe/ZnS QDs solution (5 mg dissolved in 1 mL of CHCl_3). After stirring under dark condition for 12 h at room temperature, the 1 mL of Tris-HCl buffer (pH 8.3) was added to form two phases. The addition of tetramethylammonium hydroxide pentahydrate (TMAH, 25 mg) rendered all QDs transfer to water phase, and the QDs solution was stirred for 1 h at room temperature. To remove excess of free surface ligands and base, the QDs solution was washed with chloroform, and the product was purified by dialyzing twice with Amicon Ultra-15

centrifugal filter (NMWL of 50 kDa) and characterized by TEM and FTIR (Fig. S4 and S5, ESI†).

In the study of FRET, the synthesized QDCE and RBCE was used as an energy donor and acceptor respectively. The absorption maximum of QDCE and RBCE was found to be ~515 and 554 nm respectively. The fluorescence spectrum of QDCE-RBCE conjugate exhibits dual emissions at a visible wavelength range of ~530 and 575 nm corresponding to the QDCE and RBCE moieties respectively. Fig. 1 shows the fluorescence spectra of QDCE, RBCE and QDCE-RBCE conjugate in Tris-HCl pH 8.3 buffer solution. When the QDCE and RBCE were mixed together in pH 8.3 buffer solution, the fluorescence intensity of QDCE was found to decrease whereas the fluorescence intensity of RBCE was found to increase. There are two essential features responsible for energy transfer process such as (a) the distance between the energy donor and acceptor, and (b) the spectral overlap between the emission spectrum of the energy donor and the absorption spectrum of the energy acceptor.³⁴ In the present study, it is observed that the strong spectral overlap between the absorption spectrum of RBCE and the emission spectrum of QDCE (inset Fig. 1). Hence, the observed fluorescence quenching and enhancement is attributed to the energy transfer from QDCE to RBCE. The study of FRET based metal ion selectivity was performed using fluorescence titration method. Fluorescence titration of QDCE-RBCE conjugate with different concentration of K⁺ ion in pH 8.3 buffer solution was carried out (Fig. 2). Interestingly, addition of K⁺ ion facilitates the FRET process. Both crown ether attached with quantum dot and rhodamine B moieties show reactive with K⁺ ion.

It was found that a slight red shift (~4 nm) along with an enhancement of fluorescence intensity at 575 nm corresponding to RBCE whereas decreases in the fluorescence intensity at 530 nm corresponding to QDCE with increasing concentration of K⁺ ion. On the contrary, the absorption bands of QDCE-RBCE conjugate (~515 and 554 nm) remains unchanged on the addition of K⁺ ion. These

results confirm that the FRET process is more feasible by the presence of K^+ ion in QDCE-RBCE conjugate system. Moreover, the energy transfer may take place in an excited state rather than in ground state. To further evidence for FRET, we have carried out the absorption and fluorescence measurements in varying the concentration of K^+ ion with non-conjugate systems (sole QDCE and RBCE). In both the systems, the absorption and fluorescence spectra does not much affected even in the presence of highest concentration of K^+ ion (Fig. S6, ESI†). This result reveals that the observed fluorescence intensity changes in the conjugate system is merely due to FRET between QDCE and RBCE. The time-resolved fluorescence measurements were carried out by measuring the fluorescence decay of QDCE-RBCE conjugate in the absence and presence of K^+ ion to characterize the energy transfer. The fluorescence decays were fitted well with tri-exponential function. The fluorescence lifetimes of QDCE-RBCE conjugate in an absence of K^+ ion, were found to be 2.8 (τ_1), 7.3 (τ_2) and 19.2 ns (τ_3) with an average lifetime of 12.1 ns. In the presence of K^+ ion (1 mM), fluorescence lifetimes were found to be 3.1 (τ_1), 6.8 (τ_2) and 17.8 ns (τ_3) with an average lifetime of 10.6 ns. This result shows that the energy donor QDCE lifetimes (τ_2 and τ_3) were reduced and the energy acceptor RBCE lifetime (τ_1) was increased in the presence of K^+ ion. Thus, the fluorescence lifetime studies indicate the non-radiative energy transfer from QDCE to RBCE.³⁵

Several positive charged metal ions form stable chelation complexes by strongly bind with crown ethers.^{18d,36,37} The affinity of the crown ether with metal ions is mainly influenced by the denticity of the polyether. Due to the strong binding affinity between the K^+ ion and crown ether moieties in QDCE and RBCE, sandwich complex of crown ethers with K^+ is formed.^{18a,18d,21} Consequently both the QD and rhodamine dye moieties are located in close proximity to each other which leads to FRET between QDCE and RBCE. The stoichiometry of interaction of QDCE-RBCE conjugate with K^+ ion was determined by Job's plot analysis³⁸ based on the changes in the fluorescence intensity. The Job's plot shows the maximum changes at the mole

fraction of about 0.5, which indicates 1:1 interaction of K^+ ion with QDCE-RBCE conjugate (Fig. 3). The process of energy transfer and binding mode of K^+ ion with QDCE-RBCE conjugate is depicted in Scheme 3. Initially the conjugate of QDCE-RBCE was formed due to electrostatic interaction between QDCE and RBCE. The conjugation induced a FRET from QDCE to RBCE as a result of the overlapping between emission spectrum of QDCE and absorption spectrum of RBCE. Then introducing metal ions into QDCE-RBCE conjugate system, metal ion forms a sandwich complex with crown ethers (each one of QDCE and RBCE). Due to metal ion trapped by crown ethers, the QDCE and RBCE moieties are located closely to each other which leads to more effective of FRET process. The detection limit was determined on the relation $3(\sigma/\text{slope})$, where σ is the standard deviation of the response. The detection limit of 4.3×10^{-6} M was determined from a linear correlation observed over the concentration range of 0 – 50 μM . This sensor apparently shows a high selectivity and sensitivity for the detection of K^+ ion. For comparison, the detection limit of 10 μM for K^+ ion was estimated based on an ion-selective crown ether and energy transfer from carbon dots to graphene,^{17a} and of 16 μM was recognized by benzo-15-crown-5 fluoroionophore/ γ -cyclodextrin complex sensors.^{18e}

To gain more insight into the FRET based metal ion selectivity, we performed similar fluorescence measurements for a series of metal ions (alkali metal ions such as Li^+ , Na^+ , Rb^+ and alkaline-earth metal ions like Mg^{2+} , Ca^{2+} , Sr^{2+} , Ba^{2+}) with QDCE-RBCE conjugate under identical experimental conditions (Fig. S7, ESI†). Interestingly, addition of Na^+ , Mg^{2+} and Ca^{2+} metal ions showed considerable effects in selectivity and energy transfer process, which is evident from the metal ion selectivity plot. Binding affinity of crown ethers mainly depends on the ionic size and coordination number of the metal ion. For instance calcium ions generally bind to oxygen atoms and their preferred coordination numbers range from 6 to 8.³⁹ So calcium ion may not be strongly bind with 15-crown-5-ether. The selectivity plot ($\Delta F = F - F_0$ versus $[\text{M}^{n+}]$) of QDEC-RBCE conjugate towards different metal ions is

shown in Fig. 4. F_0 and F are the fluorescence intensity ratio of (F_{575}/F_{530}) in the absence and presence of metal ion respectively. Addition of other metal ions such as Li^+ , Rb^+ , Sr^{2+} and Ba^{2+} causes the FRET process to be weakened.

The efficiency of FRET strongly depends on the separation distance between the QDCE donor and RBCE acceptor moieties. The energy transfer efficiency³⁴ was calculated using the following equation (1)

$$E = \frac{R_0^6}{R_0^6 + r^6} \quad (1)$$

in which R_0 is the Forster distance and r is distance between donor and acceptor. The Forster distance was estimated based on following equation (2),

$$R_0^6 = 8.79 \times 10^{23} (k^2 n^{-4} Q_D J(\lambda)) \text{ (in } \text{\AA}^6) \quad (2)$$

where Q_D is the quantum yield of the donor in the absence of the acceptor, n is the refractive index of the medium, k^2 is the orientation factor and generally assumed to be equal to 2/3, and $J(\lambda)$ is the overlap integral, which expresses the degree of spectral overlap between the donor emission and acceptor absorption. Table 1 shows the values of calculated distance between donor and acceptor and Forster distance for all metal ion systems. The calculated distance between donor and acceptor (r) is 46.12 Å for an above system, which is shorter distance than that of other metal ion sensing systems. The Forster distance was found to be 44.34 Å for QDCE-RBCE- K^+ ion sensing system. This calculated Forster distance was found to be lower compared to previously reported values.⁴⁰⁻⁴² Freeman *et al.* have reported the calculated R_0 value of 53.0 Å for the FRET between CdSe/ZnS QDs and rhodamine B dye.⁴⁰ Recently, Hu *et al.* have reported the R_0 value of 41.0 Å for the system of QDs and R6G derivative mercury conjugate which is close to our R_0 value.⁴³ The calculated efficiency of FRET is shown in Fig. 5. The FRET efficiency of QDCE-RBCE/metal ion systems was found to be 44.13, 34.30, 24.21, 26.32 and 1.80% for K^+ , Mg^{2+} , Na^+ , Ca^{2+} and Ba^{2+} respectively. K^+ ion exhibits the higher efficiency of FRET compared with that of all other metal ions. This results further reveal that the donor moiety of

QDCE and acceptor moiety of RBCE brought in close proximity due to the formation of sandwich complex of crown ethers with K^+ ion which enhances the FRET efficiency.

The rate constant of energy transfer [$k_{ET}(r)$] between QDCE and RBCE in the presence of metal ions was calculated by using following equation³⁴ and the values are compiled in Table 1.

$$k_{ET}(r) = \frac{1}{\tau_D} \left(\frac{R_0}{r} \right)^6 \quad (3)$$

where τ_D is the fluorescence lifetime of the donor in the absence of the acceptor. The $k_{ET}(r)$ was found to be $5.55 \times 10^7 \text{ s}^{-1}$ for K^+ ion and the rate constant of energy transfer decreases upon addition of other metal ions. For example, the rate constant for Ba^{2+} ion system was found to be $0.13 \times 10^7 \text{ s}^{-1}$. The rate of energy transfer depends on the distance between the donor and acceptor, and spectral overlap. In this present systems, the calculated higher and lower rate constant values respectively for K^+ and Ba^{2+} systems are well evidence for the observed results of distance between the donor and acceptor ($r = 46.12 \text{ \AA}$ for K^+ and 90.10 \AA for Ba^{2+}). This result confirms that the energy transfer is more feasible when an addition of K^+ ion to QDCE-RBCE conjugate.

Finally, we have estimated the binding constant ($\log K$) by using the Benesi–Hildebrand method.⁴⁴ The Benesi–Hildebrand plot of $1/(F - F_0)$ versus $1/[M^{n+}]$ exhibits a straight line, which is further confirms the 1:1 stoichiometry (Fig. S8, ESI†). The binding constant values are determined by dividing the intercept by the slope of the straight line. The $\log K$ was estimated to be 3.09, 2.77, 2.45, 1.90, 1.77, and 1.62 for K^+ , Mg^{2+} , Na^+ , Ca^{2+} , Rb^+ and Li^+ metal ions respectively. The binding constant of other metal ions (Sr^{2+} , Ba^{2+}) could not be estimated due to minor changes in the corresponding fluorescence spectra. Based on all results, it may conclude that the synthesized fluorescent QDCE and RBCE performs as a great selective FRET-based ratiometric fluorescence probe towards K^+ ion.

Conclusions

We have established a FRET based metal ion sensors. A varying metal ion concentrations was introduced to the FRET sensor system, FRET from QDCE to RBCE was induced by metal ions. Efficiency of energy transfer depends on the affinity between metal ions and crown ether functionalized with QDCE/RBCE. The sensor shows excellent selectivity towards K^+ ion resulting in the enhanced FRET between QDCE and RBCE conjugate, which evident from the observed higher efficiency and rate constant of FRET for K^+ ions compared with that of other metal ions. The stoichiometry of interaction of QDCE-RBCE conjugate with K^+ ion was found to be 1:1 which reveals that the K^+ ion formed sandwich like complex with crown ethers of QDCE-RBCE conjugate. Due to high selectivity for K^+ , the QDCE-RBCE conjugate sensor system have good potential for an application in the determination of this metal ion in biological systems.

Experimental Section

Materials and Methods

All commercially available organic reagents were used without further purification. Dichloromethane was distilled from CaH_2 under N_2 . Flash column chromatography was carried out with silica gel 60 (Merck). Thin layer chromatography was performed with silica gel 60 F254 plates purchased from Merck. The hydrophobic CdSe/ZnS QDs capped with octadecylamine were obtained from Ocean NanoTech, USA, and used as without further purification.

UV–Visible absorption spectra were recorded on a Thermo Scientific evolution 220 spectrophotometer. Fluorescence spectra were recorded on a Perkin-Elmer LS45 spectrophotometer. Fluorescence decays were recorded by using the time-correlated single-photon counting technique as reported elsewhere.⁴⁵ 1H NMR and ^{13}C NMR spectra were recorded on a Bruker DPX 400MHz NMR spectrometer in deuterated

solvents. All NMR spectra were assigned, and the chemical shifts are reported in ppm downfield relative to the chemical shift. Electrospray ionization mass spectrometry (ESI-MS) experiments were carried out on a Bruker microTOF-QII mass spectrometer. Infrared spectra were recorded on a Thermo Scientific Nicolet iS5 FT-IR spectrometer. TEM observations were conducted on a Hitachi H-7100 transmission electron microscope. All measurement were recorded at ambient temperature.

Characterization of RBCE and QDCE

Boc-6-Ahx-15-crown-5 [Scheme 1, (iii)]

^1H NMR (400 MHz, CDCl_3): δ = 4.53 (s, NH), 4.22-4.04 (m, 2H), 3.83-3.52 (m, 19H), 3.08 (q, 2H), 2.31 (t, 2H), 1.65-1.29 (m, 15H). ^{13}C NMR (100 MHz, CDCl_3): δ = 173.43, 79.10, 71.12, 70.93, 70.85, 70.78, 70.56, 70.44, 70.22, 64.06, 40.37, 34.06, 29.73, 28.42, 26.26, 24.55 ppm.

15-crown-5-ether attached Rhodamine B, RBCE [Scheme 1, (v)]

^1H NMR (400 MHz, CD_3OD): δ = 7.85-7.82 (m, 1H), 7.53-7.48 (m, 2H), 7.05-7.02 (m, 1H), 6.42-6.23 (m, 6H), 4.26-4.08 (m, 2H), 3.81-3.55 (m, 19H), 3.36 (q, 8H), 3.04 (m, 2H), 2.14 (t, 2H), 1.37 (t, 2H), 1.14 (t, 12H), 1.06 (tt, 4H). ^{13}C NMR (100 MHz, CD_3OD): δ = 174.73, 169.81, 154.87, 154.77, 150.38, 133.96, 132.51, 129.68, 129.49, 125.09, 123.39, 109.50, 106.50, 99.03, 77.63, 70.50, 70.37, 70.23, 70.05, 69.93, 69.80, 69.77, 69.53, 66.98, 63.46, 45.37, 41.01, 34.57, 28.87, 27.46, 25.46, 12.88 ppm. ESI-MS: m/z calcd. for $[\text{M} + \text{Na}^+]^+$ 810.4300, found 810.4289.

15-crown-5- DHLA [Scheme 2, (C)]

^1H NMR (400 MHz, CDCl_3): δ = 4.21-4.03 (m, 2H), 3.82-3.51 (m, 19H), 3.15-3.06 (m, 2H), 2.42 (sext, 1H), 2.31 (t, 2H), 1.87 (sext, 1H), 1.69-1.59 (m, 4H), 1.48-1.35 (m, 2H). ^{13}C NMR (100 MHz, CDCl_3): δ = 173.12, 70.91, 70.72, 70.62, 70.56,

70.36, 70.28, 70.21, 70.04, 63.93, 56.13, 40.03, 38.30, 34.40, 33.79, 28.52, 24.47 ppm. ESI-MS: m/z calcd. for $[M + Na^+]^+$ 461.1638, found 461.1633.

General procedure for sensing of metal ion

Metal chloride stock solutions were prepared in pH 8.3 buffer solutions, and the fluorescence titration measurements were carried out by adding small volumes (upto 5 μ l) of the metal ion to the QDCE-RBCE conjugate solution in a quartz cuvette. After an addition of metal ion to the cuvette, the solution was shaken well and kept 2 min before measurement. QDCE and RBCE stock solutions were prepared in pH 8.3 buffer solutions.

Acknowledgements

This work was supported by Ministry of Science and Technology of Taiwan, Republic of China under contract no. NSC 99-2113-M-002-010-MY3.

Electronic Supplementary Information (ESI) available: ^1H NMR, ^{13}C NMR, FTIR spectra and fluorescence spectral study figures. See DOI:

Notes and references

^a Equal contribution

*To whom correspondence should be addressed.

Department of Chemistry, National Taiwan University, Taipei 106, and Institute of Atomic and Molecular Sciences, Academia Sinica, Taipei 106, Taiwan.

Email: kclin@ntu.edu.tw; Fax: +886-2-2362-1483; Tel: +886-2-3366-1162.

- (a) W. Maret and A. Wedd, *Binding, Transport and Storage of Metal Ions in Biological Cells*, RSC, Cambridge, UK, 2014; (b) J. A. Cowan, *Inorganic biochemistry: An introduction*, Wiley-VCH, Inc., USA, 1997; (c) J. B. Ames, K. B.

- Hendricks, T. Strahl, I. G. Huttner, N. Hamasaki and J. Thorner, *Biochemistry*, 2000, **39**, 12149–12161; (d) J. C. Henquin, T. Tamagawa, M. Nenquin and M. Cogneau, *Nature*, 1983, **301**, 73–74; (e) B. Valeur and I. Leray, *Coord. Chem. Rev.*, 2000, **205**, 3–40; (f) Y. Xiang and Y. Lu, *Inorg. Chem.*, 2014, **53**, 1925–1942.
- 2 (a) J. Lee, H.-J. Kim and J. Kim, *J. Am. Chem. Soc.*, 2008, **130**, 5010–5011; (b) I. Leray, B. Valeur, F. O'Reilly, J.-L. Habib Jiwan, J.-Ph. Soumillion and B. Valeur, *Chem. Commun.*, 1999, 795–796; (c) H. Ueyama, M. Takagi and S. Takenaka, *J. Am. Chem. Soc.*, 2002, **124**, 14286–14287; (d) H. Ma, E. A. Gibson, P. J. Dittmer, R. Jimenez and A. E. Palmer, *J. Am. Chem. Soc.*, 2012, **134**, 2488–2491; (e) N. B. Sankaran, S. Nishizawa, M. Watanabe, T. Uchidaa and N. Teramae, *J. Mater. Chem.*, 2005, **15**, 2755–2761; (f) H. Wang, D. M. Wang, M. X. Gao, J. Wang and C. Z. Huang, *Anal. Methods*, 2014, **6**, 7415–7419; (g) E. Arunkumar, P. Chithra and A. Ajayaghosh, *J. Am. Chem. Soc.*, 2004, **126**, 6590–6598.
- 3 L. D. Stryer, *Biochemistry*, 3rd ed; Freeman, New York, 1988, pp 949–974.
- 4 I. Cakmak, *J. Plant Nutr. Soil Sci.*, 2005, **168**, 521–530.
- 5 P. Maser, M. Gierth and J. I. Schroeder, *Plant Soil*, 2002, **247**, 43–54.
- 6 T. Hirata, T. Terai, T. Komatsu, K. Hanaoka and T. Nagano, *Bioorg. Med. Chem. Lett.*, 2011, **21**, 6090–6093.
- 7 M. F. S. Teixeira, B. H. Freitas, P. M. Seraphim, L. O. Salmazo, M. A. Nobre and S. Lanfredi, *Proc. Chem.*, 2009, **1**, 293–296.
- 8 B. T. T. Nguyen, J. Q. Ang and C.-S. Toh, *Electrochem. Commun.*, 2009, **11**, 1861–1864.
- 9 H. Chen, Y. S. Gal and S. H. Kim, *Sens. Actuators, B*, 2008, **133**, 577–581.
- 10 B. Yu, L. Nie and S. Yao, *J. Chromatogr. B: Biomed. Sci. Appl.*, 1997, **693**, 43–49.
- 11 L. B. de Caland, E. L. C. Silveira and M. Tubino, *Anal. Chim. Acta*, 2012, **718**, 116–120.

- 12 T. Li, E. Wang and S. Dong, *Anal. Chem.*, 2010, **82**, 7576–7580.
- 13 S. Kim, H. Kim, K. H. Noh, S. H. Lee, S. K. Kim and J. S. Kim, *Talanta*, 2003, **61**, 709–716.
- 14 A. P. de Silva, H. Q. N. Gunaratne, T. Gunnlaugsson, A. J. M. Huxley, C. P. McCoy, J. T. Rademacher and T. E. Rice, *Chem. Rev.*, 1997, **97**, 1515–1566.
- 15 X. Chen, X. Tian, I. Shin and J. Yoon, *Chem. Soc. Rev.*, 2011, **40**, 4783–4804.
- 16 (a) B. Valeur, *Molecular Fluorescence. Principles and Applications*, Wiley-VCH, Weinheim, 2002; (b) F. He, Y. Tang, S. Wang, Y. Li and D. Zhu, *J. Am. Chem. Soc.*, 2005, **127**, 12343–12346; (c) J. Kim, D. T. McQuade, S. K. McHugh and T. M. Swager, *Angew. Chem., Int. Ed.*, 2000, **39**, 3868–3872; (d) H. He, M. A. Mortellaro, M. J. P. Leiner, R. J. Fraatz and J. K. Tusa, *J. Am. Chem. Soc.*, 2003, **125**, 1468–1469.
- 17 (a) W. Wei, C. Xu, J. Ren, B. Xu and X. Qu, *Chem. Commun.*, 2012, **48**, 1284–1286; (b) J. Yin, C. Li, D. Wang and S. Liu, *J. Phys. Chem. B*, 2010, **114**, 12213–12220; (c) B. Sen, M. Mukherjee, S. Pal, K. Dhara, S. K. Mandal, A. R. Khuda-Bukhsh and P. Chattopadhyay, *RSC Adv.*, 2014, **4**, 14919–14927.
- 18 (a) S.-Y. Lin, S.-W. Liu, C.-M. Lin and C.-H. Chen, *Anal. Chem.*, 2002, **74**, 330–335; (b) M.-L. Ho, J.-M. Hsieh, C.-W. Lai, H.-C. Peng, C.-C. Kang, I.-C. Wu, C.-H. Lai, Y.-C. Chen and P.-T. Chou, *J. Phys. Chem. C*, 2009, **113**, 1686–1693; (c) S. Flink, F. C. J. M. Van Veggel and D. N. Reinhoudt, *J. Phys. Chem. B*, 1999, **103**, 6515–6520; (d) G. W. Gokel, W. M. Leevy and M. E. Weber, *Chem. Rev.*, 2004, **104**, 2723–2750; (e) A. Yamauchi, T. Hayashita, A. Kato, S. Nishizawa, M. Watanabe and N. Teramae, *Anal. Chem.*, 2000, **72**, 5841–5846.
- 19 (a) A. Yamauchi, T. Hayashita, S. Nishizawa, M. Watanabe and N. Teramae, *J. Am. Chem. Soc.*, 1999, **121**, 2319–2320; (b) A. P. Desilva, H. Q. N. Gunaratne and K. R. A. S. Sandanayake, *Tetrahedron Lett.*, 1990, **31**, 5193–5196; (c) M. Baruah, W. Qin, R. A. L. Vallee, D. Beljonne, T. Rohand, W. Dehaen and N. Boens, *Org.*

- Lett.*, 2005, **7**, 4377–4380; (d) K. H. Mühling and B. Sattelmacher, *J. Exp. Bot.* 1997, **48**, 1609–1614.
- 20 M. J. Ruedas-Rama, X. Wang and E. A. H. Hall, *Chem. Commun.*, 2007, 1544–1546.
- 21 C-Y. Chen, C-T. Cheng, C-W. Lai, P-W. Wu, K-C. Wu, P-T. Chou, Y-H. Chou and H-T. Chiu, *Chem. Commun.*, 2006, 263–265.
- 22 W. R. Algar and U. J. Krull, *Anal. Bioanal. Chem.* 2008, **391**, 1609–1618.
- 23 G. Chen, F. Song, X. Xiong and X. Peng, *Ind. Eng. Chem. Res.* 2013, **52**, 11228–11245.
- 24 D. Liu, T. Pang, K. Ma, W. Jiang and X. Bao, *RSC Adv.*, 2014, **4**, 2563–2567.
- 25 X. Zhang, Y. Shiraishi and T. Hirai, *Tetrahedron Lett.*, 2008, **49**, 4178–4181.
- 26 W. Yuanboonlim, W. Siripornnoppakhun, N. Niamnont, P. Rashatasakhon, T. Vilaivan and M. Sukwattanasinitt, *Biosens. Bioelectron.*, 2012, **33**, 17–22.
- 27 C. Shi, H. Gu and C. Ma, *Anal. Biochem.*, 2010, **400**, 99–102.
- 28 Y. Liu, B. Li, D. Cheng and X. Duan, *Microchem. J.*, 2011, **99**, 503–507.
- 29 X. Fan, H. Li, J. Zhao, F. Lin, L. Zhang, Y. Zhang and S. Yao, *Talanta*, 2012, **89**, 57–62.
- 30 Z. Chen, J. Guo, H. Ma, T. Zhoua and X. Lia, *Anal. Methods*, 2014, **6**, 8018–8021.
- 31 Z. Chen, Y. Huang, X. Li, T. Zhou, H. Ma, H. Qiang and Y. Liu, *Anal. Chim. Acta*, 2013, **787**, 189–192.
- 32 N. Gavande, H.-L. Kim, M. R. Doddareddy, G. A. R. Johnston, M. Chebib and J. R. Hanrahan, *ACS Med. Chem. Lett.*, 2013, **4**, 402–407.
- 33 H. Mattoussi, J. M. Mauro, E. R. Goldman, G. P. Anderson, V. C. Sundar, F. V. Milkulec and M. G. Bawendi, *J. Am. Chem. Soc.*, 2000, **122**, 12142–12150.
- 34 J. R. Lakowicz, *Principles of Fluorescence Spectroscopy*, 3rd ed; Springer: New York, 2006.
- 35 E. Lee, C. Kim and J. Jang, *Chem. Eur. J.*, 2013, **19**, 10280–10286.
- 36 K. Rurack, W. Rettig, and U. Resch-Genger, *Chem. Commun.*, 2000, 407–408.

- 37 C. Han and H. Li, *Anal. Bioanal. Chem.*, 2010, **397**, 1437–1444.
- 38 P. Job, *Ann. Chem.*, 1928, **9**, 113–203.
- 39 A. K. Katz, J. P. Glusker, S. A. Beebe and C. W. Bock, *J. Am. Chem. Soc.*, 1996, **118**, 5752–5763.
- 40 R. Freeman, T. Finder, L. Bahshi and I. Willner, *Nano lett.*, 2009, **9**, 2073–2076.
- 41 S. Nagatoishi, T. Nojima, E. Galezowska, A. Gluszynska, B. Juskowiak and S. Takenaka, *Anal. Chim. Acta*, 2007, **581**, 125–131.
- 42 J.-L. Mergny and J.-C. Maurizot, *ChemBioChem*, 2001, **2**, 124–132.
- 43 B. Hu, L.-L. Hu, M.-L. Chen and J.-H. Wang, *Biosens. Bioelectron.*, 2013, **49**, 499–505.
- 44 H. A. Benesi and J. H. Hildebrand, *J. Am. Chem. Soc.*, 1949, **71**, 2703–2707.
- 45 C.-L. Chang, P.-Y. Tsai, Y.-P. Chang and K.-C. Lin, *ChemPhysChem*, 2012, **13**, 2711–2720.

Figure and Scheme captions

Fig. 1 Fluorescence spectra of QDCE, RBCE and QDCE-RBCE conjugate in pH 8.3 buffer. $\lambda_{\text{ex}} = 375$ nm. Inset: Spectral overlap between emission spectrum of QDCE and absorption spectrum of RBCE.

Fig. 2 Fluorescence spectra of QDCE-RBCE conjugate with different concentration of K^+ ion (0 to 2.5×10^{-3} M) in pH 8.3 buffer. $\lambda_{\text{ex}} = 375$ nm.

Fig. 3 Job's plot for the binding of K^+ ion with QDCE-RBCE conjugate. Mole fraction = $[\text{conjugate}] / ([\text{conjugate}] + [\text{K}^+ \text{ ion}])$.

Fig. 4 Metal ion selectivity plot of QDCE-RBCE conjugate upon addition of different metal ions in pH 8.3 buffer.

Fig. 5 FRET efficiency of QDCE-RBCE conjugate with different metal ions in pH 8.3 buffer.

Table 1 Forster radius, rate constant and efficiency of energy transfer for QDCE-RBCE conjugate with metal ion systems.

Scheme 1 The synthetic procedure of 15-Crown-5-ether attached rhodamine B.

Scheme 2 The synthetic procedure of 15-Crown-5-ether capped CdSe/ZnS QDs.

Scheme 3 Schematic representation of FRET between QDCE and RBCE.

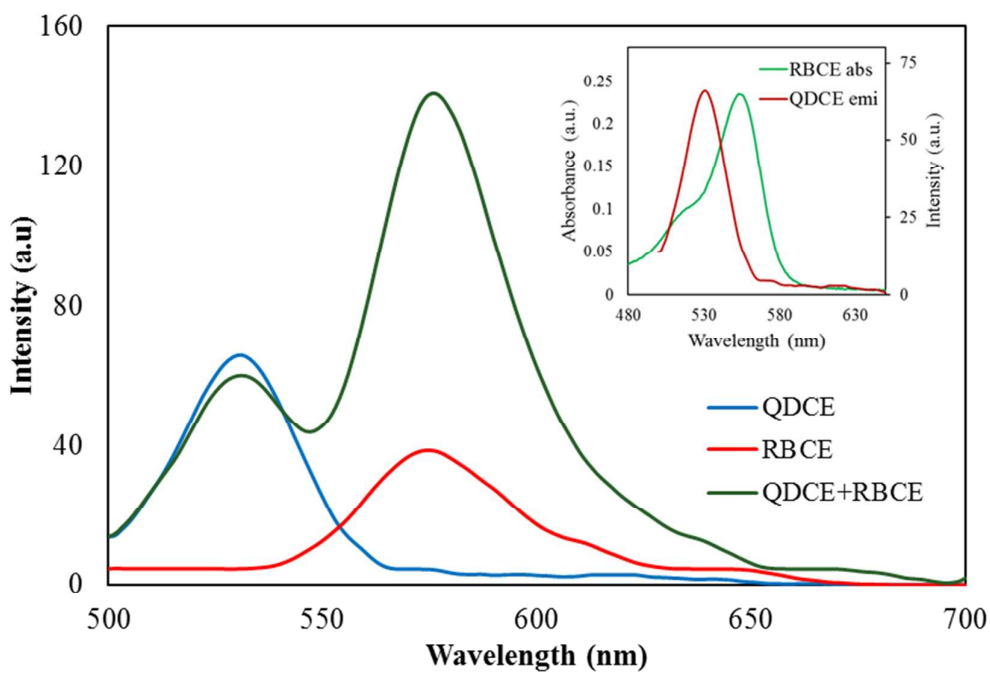


Fig. 1 Fluorescence spectra of QDCE, RBCE and QDCE-RBCE conjugate in pH 8.3 buffer. $\lambda_{\text{ex}} = 375$ nm. Inset: Spectral overlap between emission spectrum of QDCE and absorption spectrum of RBCE.

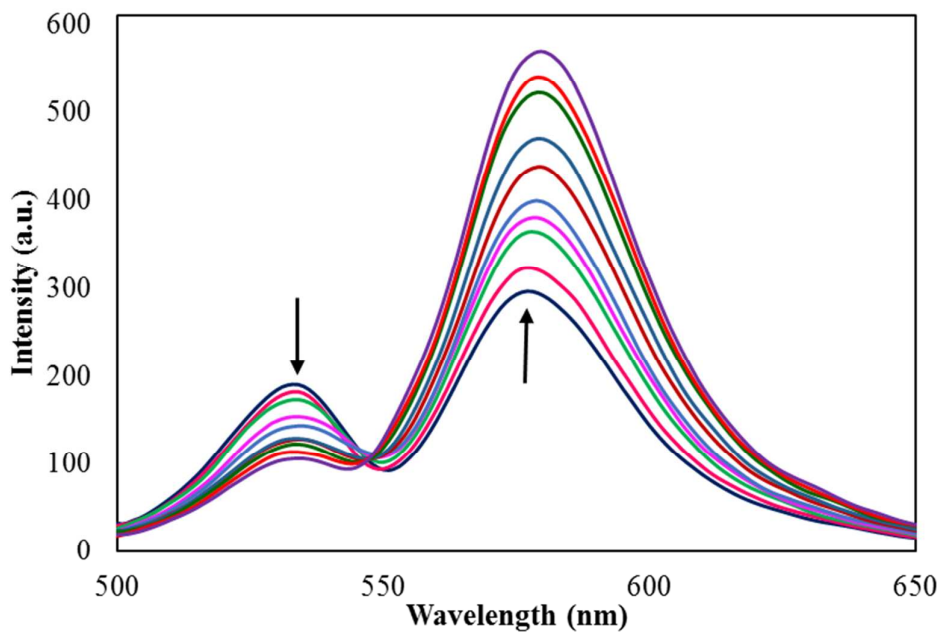


Fig. 2 Fluorescence spectra of QDCE-RBCE conjugate with different concentration of K⁺ ion (0 to 2.5×10^{-3} M) in pH 8.3 buffer. $\lambda_{\text{ex}} = 375$ nm.

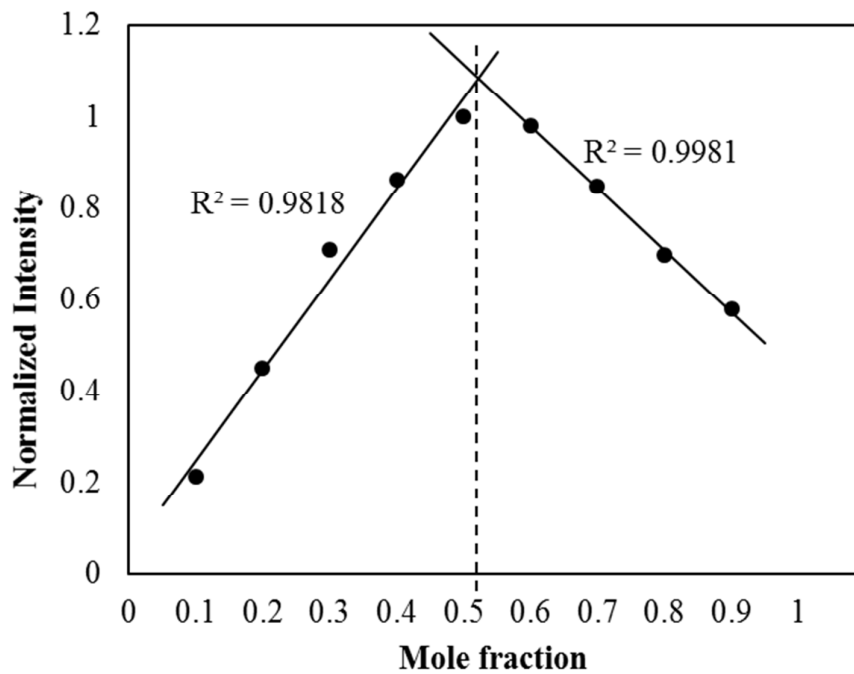


Fig. 3 Job's plot for the binding of K⁺ ion with QDCE-RBCE conjugate. Mole fraction = [conjugate] / ([conjugate] + [K⁺ ion]).

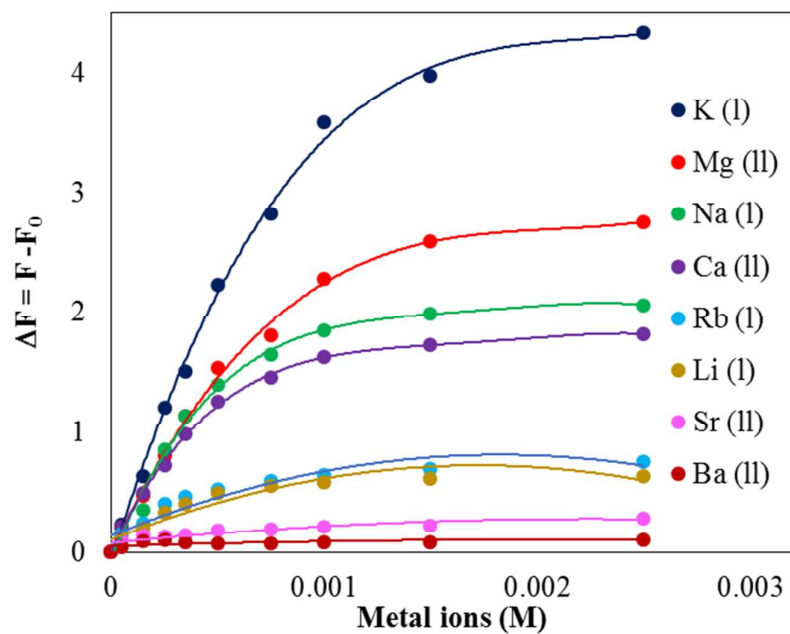


Fig. 4 Metal ion selectivity plot of QDCE-RBCE conjugate upon addition of different metal ions in pH 8.3 buffer.

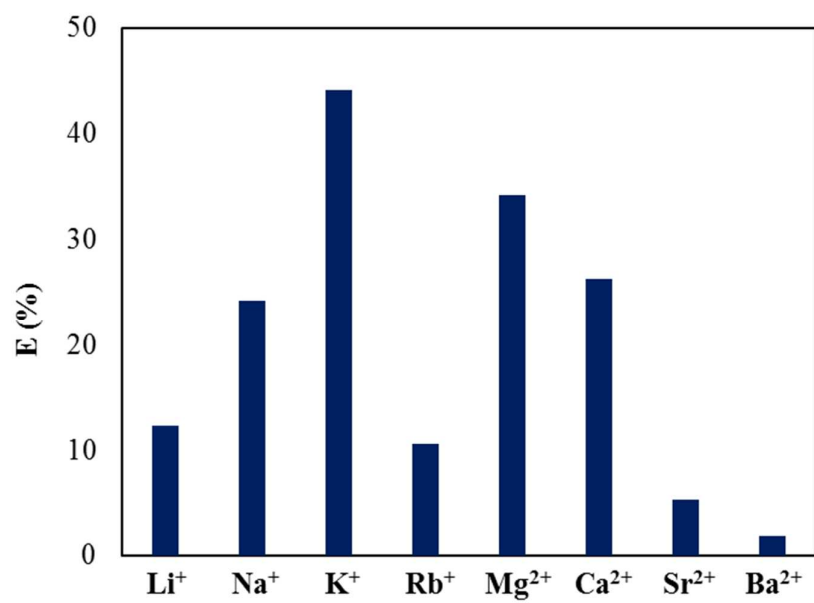
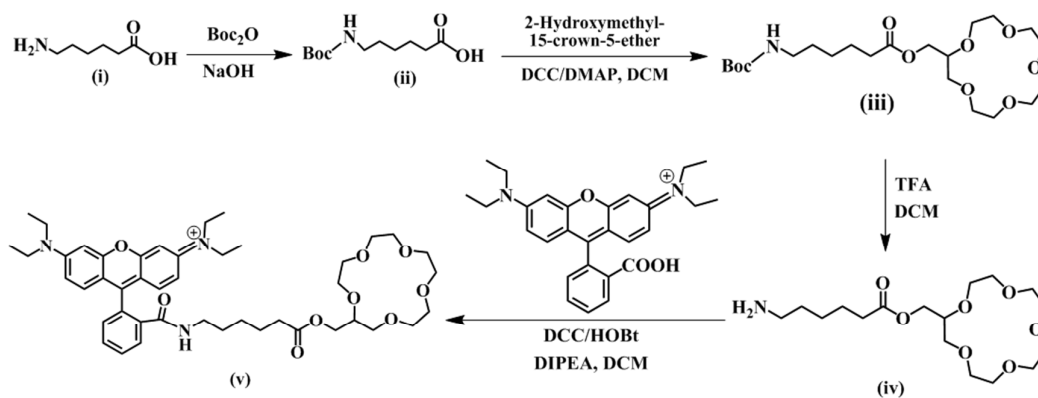


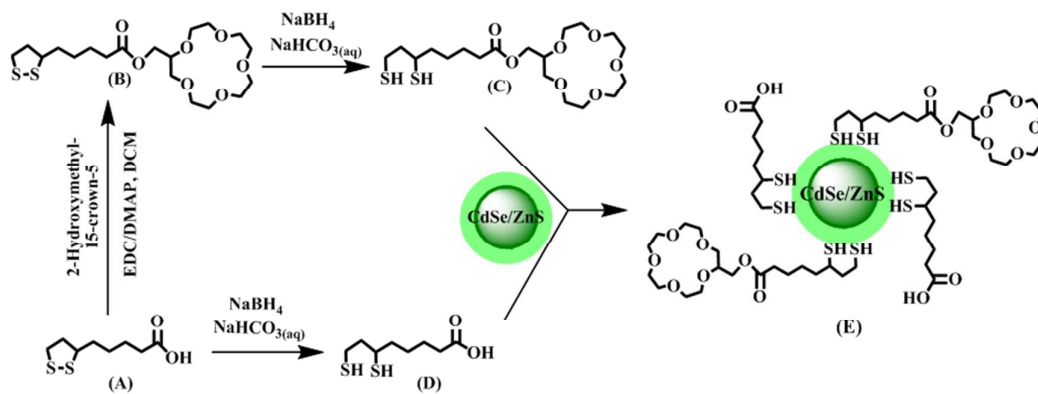
Fig. 5 FRET efficiency of QDCE-RBCE conjugate with different metal ions in pH 8.3 buffer.

Table 1: Forster radius, rate constant and efficiency of energy transfer for QDCE-RBCE conjugate with metal ion systems.

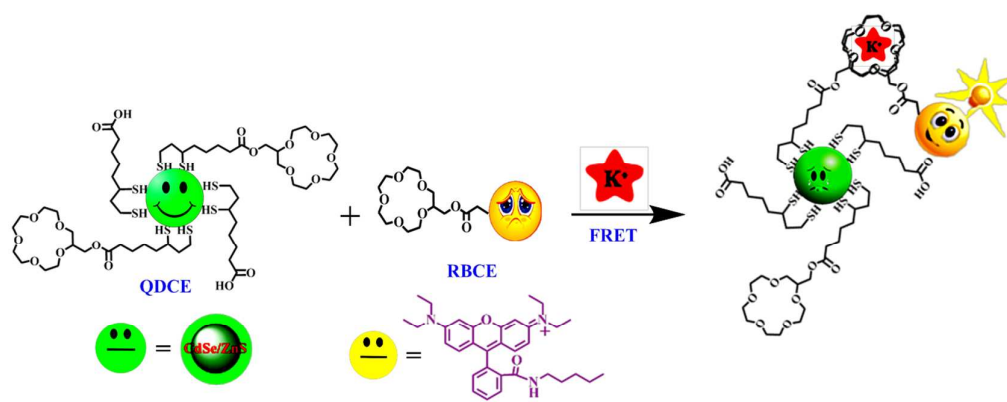
Metal ions	R₀ (Å)	r (Å)	k_{ET} (r) [×10⁷ s⁻¹]	E (%)
Li ⁺	45.06	62.46	0.99	12.36
Na ⁺	44.19	53.46	2.24	24.21
K ⁺	44.34	46.12	5.55	44.13
Rb ⁺	46.06	65.8	0.82	10.53
Mg ²⁺	44.03	49.07	3.67	34.30
Ca ²⁺	44.75	53.16	2.50	26.32
Sr ²⁺	46.43	74.94	0.40	5.40
Ba ²⁺	46.26	90.10	0.13	1.80



Scheme 1 The synthetic procedure of 15-Crown-5-ether attached rhodamine B.



Scheme 2 The synthetic procedure of 15-Crown-5-ether capped CdSe/ZnS QDs.



Scheme 3 Schematic representation of FRET between QDCE and RBCE.